

A study on the magnetic behaviour of polymorphic YbFe_6Ge_6

This article has been downloaded from IOPscience. Please scroll down to see the full text article.

2010 J. Phys.: Condens. Matter 22 016009

(<http://iopscience.iop.org/0953-8984/22/1/016009>)

View [the table of contents for this issue](#), or go to the [journal homepage](#) for more

Download details:

IP Address: 129.252.86.83

The article was downloaded on 30/05/2010 at 06:30

Please note that [terms and conditions apply](#).

A study on the magnetic behaviour of polymorphic YbFe_6Ge_6

J M Cadogan¹ and D H Ryan²

¹ Department of Physics and Astronomy, University of Manitoba, Winnipeg, MB, R3T 2N2, Canada

² Department of Physics, McGill University, Montreal, QC, H3A 2T8, Canada

E-mail: cadogan@physics.umanitoba.ca

Received 30 September 2009, in final form 9 November 2009

Published 8 December 2009

Online at stacks.iop.org/JPhysCM/22/016009

Abstract

The intermetallic compound YbFe_6Ge_6 adopts two very closely related hexagonal crystal structures, HfFe_6Ge_6 -type and YCo_6Ge_6 -type. In both structures the Fe sublattice orders antiferromagnetically at 485(2) K. The Yb sublattice does not order magnetically, down to 1.5 K. In the HfFe_6Ge_6 -type structure, the Fe magnetic moments undergo a spin reorientation away from the *C*-axis upon cooling, commencing at around 60 K, whereas in the YCo_6Ge_6 -type structure the Fe moments remain ordered along the *C*-axis, or quite close to it.

(Some figures in this article are in colour only in the electronic version)

1. Introduction

The rare-earth (R) and Fe sublattices in the RFe_6Ge_6 and RFe_6Sn_6 intermetallic compounds exhibit independent magnetic behaviour ([1] and references therein). The Fe sublattice orders antiferromagnetically with a Néel temperature which remains essentially constant across a series at ~ 485 K for RFe_6Ge_6 or ~ 555 K for RFe_6Sn_6 . For $\text{R} = \text{Gd-Er}$, the R sublattice orders with Curie temperatures ranging from a high of 45 K in GdFe_6Sn_6 to 3 K in ErFe_6Ge_6 .

The layered nature of the crystal structures adopted by the RFe_6Ge_6 and RFe_6Sn_6 compounds provides a simple framework within which this magnetic independence can be understood. The RFe_6Ge_6 and RFe_6Sn_6 compounds crystallize in either orthorhombic or hexagonal structures which are derived from the hexagonal B35 structure of the parent FeGe or FeSn compounds [2]. In the RFe_6Ge_6 and RFe_6Sn_6 compounds the R atoms lie midway between adjacent hexagonal Fe planes of FeGe or FeSn and the resulting exchange interaction at the R sites, due to the neighbouring Fe planes, is zero [3].

The YbFe_6Ge_6 compound was first reported by Buchholz and Schuster [4] who determined its crystal structure to be the ordered hexagonal HfFe_6Ge_6 -type structure in which the crystal cell is doubled along the hexagonal *C*-axis relative to the underlying FeGe basis, with full site-occupancies. Later, Dzyanyi *et al* [5] reported the crystal structure to be the hexagonal YCo_6Ge_6 -type in which the Yb ions have a 50% occupancy of the 1a site with a cell size almost the same as

the FeGe compound. A 50% occupancy was also found at one of the Ge sites. In a comprehensive study of the RFe_6Ge_6 and RFe_6Sn_6 series, Venturini *et al* [6] reported a HfFe_6Ge_6 -type structure for YbFe_6Ge_6 . For a detailed description of the crystallography of the RFe_6Ge_6 and RFe_6Sn_6 systems we refer the reader to the review by Venturini [7]. Throughout this paper we will use the notations ‘H-type’ and ‘Y-type’ to refer to the HfFe_6Ge_6 -type and YCo_6Ge_6 -type structures of YbFe_6Ge_6 , respectively.

The magnetism of the FeGe basis has been the subject of extensive investigation over the past four decades. This work encompasses ^{57}Fe Mössbauer spectroscopy [8–10], magnetic measurements [11–13], neutron diffraction [14–16] and theoretical studies [17, 18]. The Fe sublattice orders antiferromagnetically below 410 K with the Fe moments aligned along the hexagonal *C*-axis. Below 55 K, the Fe moments deviate from the crystal *C*-axis and form a ‘double-cone’ structure [11, 14–16].

Spin reorientations of the type observed in FeGe are scarce in the RFe_6Ge_6 and RFe_6Sn_6 systems. In 2000, Mazet and Malaman [19] reported a study of the magnetic structure of nominally H-type YbFe_6Ge_6 based on ^{57}Fe Mössbauer spectroscopy and neutron powder diffraction measurements. They reported that the magnetic structure of the Fe sublattice is a collinear *C*-axis antiferromagnet below 491 K but a fraction of the Fe moments deviate away from the *C*-axis upon cooling below about 85 K. The ^{57}Fe Mössbauer spectra obtained above this spin-reorientation temperature, but below

the Néel temperature, were fitted as a single, magnetically-split sextet. Below 85 K, the reoriented Fe moments were represented by three, equal-area magnetic sextets in the ^{57}Fe Mössbauer spectra and the reoriented proportion was claimed to be temperature-dependent, reaching 82% at 4.2 K. A fourth magnetic sextet, with a relative subspectral area of 18% at 4.2 K, was interpreted as representing Fe moments that had remained along the crystal C -axis. The Fe atoms in H-type YbFe_6Ge_6 occupy a single, six-fold crystallographic site (6i) which makes the observation of the unusual unreoriented subspectral area of 18% hard to reconcile with the crystallography.

Mazet and Malaman [19] also found it necessary to introduce a partial redistribution of the Yb and Ge(2e) atoms into other sites in order to fit certain characteristic peaks in their diffraction patterns. In particular, the Yb atoms were split into a 73% occupancy of the 1a site and a 27% occupancy of the 1b site. Once again, this is hard to reconcile with the ordered crystallographic nature of the H-type structure.

In this paper we show that the observation of two closely related crystallographic forms of YbFe_6Ge_6 provides a ready explanation of the results presented by Mazet and Malaman [19]. We find that a major reorientation of the Fe sublattice magnetic order only occurs in H-type YbFe_6Ge_6 . By contrast, the Fe moments in Y-type YbFe_6Ge_6 remain ordered along, or quite close to, the hexagonal C -axis.

2. Experimental methods

The YbFe_6Ge_6 samples were prepared by arc-melting stoichiometric amounts of the pure elements (Yb: 99.9%, Fe: 99.95%, Ge: 99.999%) under Ti-gettered argon, allowing an excess of 20 wt% Yb to account for the inevitable Yb boil-off in the arc-furnace. The arc-melted ingots were annealed at 900 °C for two weeks, sealed under vacuum in quartz tubes. Conventional arc-melting followed by annealing generally leads to the YCo_6Ge_6 -type phase, although one of our preparations by this method did yield the HfFe_6Ge_6 -type phase, and Mazet and Malaman [19] appear to have obtained a mixture of the two forms by reacting pressed pellets of the pure elements at 750 °C. The only method that consistently yields H-type YbFe_6Ge_6 involves growth from a tin flux [20]. We are currently exploring this technique.

Samples were characterized by powder x-ray diffraction with Cu $K\alpha$ radiation on an automated Nicolet–Stoe diffractometer. The Néel temperature of the Fe sublattice in YbFe_6Ge_6 was measured by differential scanning calorimetry on a Perkin–Elmer DSC-7, using the heat capacity peak at T_N as the signature of the magnetic ordering. AC-susceptibility measurements were made on a LakeShore 7130 susceptometer at a frequency of 137 Hz and an ac magnetic field of 700 A m^{-1} (rms). We observed no sign of magnetic ordering of the Yb sublattice down to 4 K in our neutron powder diffraction work, consistent with the report by Mazet and Malaman that the Yb sublattice does not order down to 1.5 K [19].

^{57}Fe Mössbauer spectroscopy was carried out in transmission mode with a $^{57}\text{CoRh}$ source. ^{170}Yb Mössbauer spectroscopy was also carried out in transmission mode with

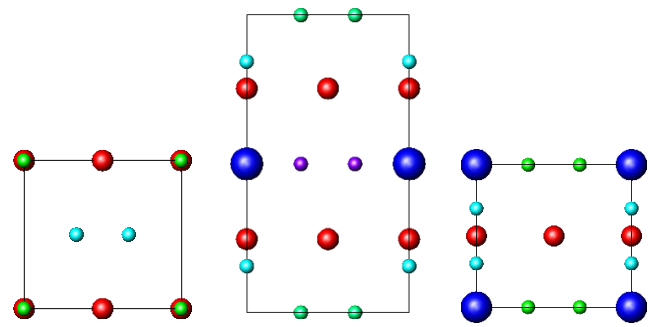


Figure 1. Crystal structures of FeGe, H-type and Y-type YbFe_6Ge_6 , shown as projections along the [100] direction. The atomic symbols decrease in size in the order Yb (large dark blue) > Fe (medium red) > Ge (small green, purple and cyan).

a 20 mCi ^{170}Tm source that was prepared by neutron activation of ~ 25 mg of Tm as a 10 wt% alloy in aluminium. All Mössbauer spectra were least-squares fitted by diagonalization of the full nuclear hyperfine Hamiltonian. We refer the reader to our review of R-isotope Mössbauer spectroscopy for details of the ^{170}Yb Mössbauer transition [21].

Neutron diffraction experiments were carried out on the C2 multi-wire powder diffractometer (DUALSPEC) at the NRU reactor, Canadian Neutron Beam Centre, Chalk River, Ontario. Temperatures down to 3.7 K were obtained using a closed-cycle refrigerator. The neutron wavelength was 1.5049(1) Å and all refinements of the neutron and x-ray diffraction patterns employed the FULLPROF/WinPlotr package [22, 23]. Finally, all crystal structure diagrams were drawn using the ATOMS package by Shape Software.

3. Results and discussion

3.1. Structural

The annealed samples of YbFe_6Ge_6 contained traces of Yb_2O_3 and YbFe_2Ge_2 in the total amount of ~ 3 wt%, as estimated from the refinements of the x-ray and neutron diffraction patterns. The H-type and Y-type hexagonal crystal structures of YbFe_6Ge_6 are closely related to each other and both have the $P6/mmm$ (#191) space group. We were unable to avoid any ‘cross-contamination’ between the H-type and Y-type phases and our diffraction pattern refinements suggest that the level of cross-contamination in both the nominal Y-type and nominal H-type samples amounts to about 5 wt%.

The lattice parameters (at 295 K) are $a = 5.122(3)$ Å and $c = 4.071(3)$ Å for the Y-type YbFe_6Ge_6 phase and $a = 5.122(3)$ Å and $c = 8.141(4)$ Å for the H-type phase. The H-type and Y-type crystal structures of YbFe_6Ge_6 , along with that of FeGe for comparison, are shown in figures 1–3. The key point illustrated by these diagrams is the doubling of the crystal cell along the C -axis in H-type YbFe_6Ge_6 , relative to the cells of FeGe and Y-type YbFe_6Ge_6 . The refined crystallographic data for the Yb, Fe and Ge sites in the two crystallographic forms of YbFe_6Ge_6 are given in table 1.

In figure 4 we show the ac-susceptibility of H-type YbFe_6Ge_6 . The spin reorientation of the Fe sublattice produces

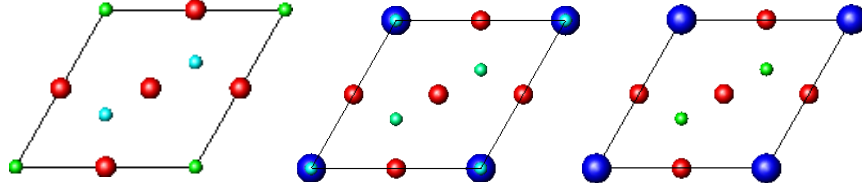


Figure 2. Crystal structures of FeGe, H-type and Y-type YbFe_6Ge_6 , shown as projections along the [001] direction (atomic symbols as in figure 1).

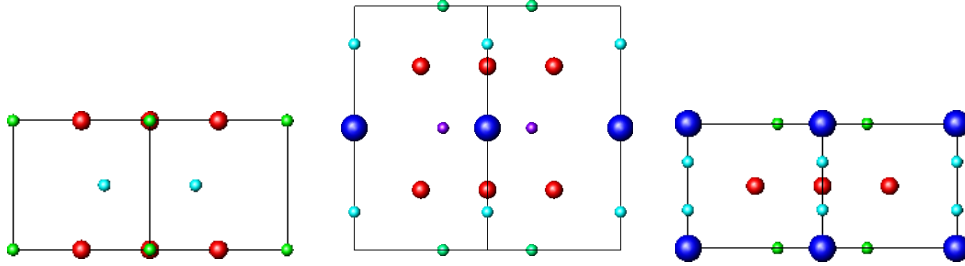


Figure 3. Crystal structures of FeGe, H-type and Y-type YbFe_6Ge_6 , shown as projections along the [110] direction (atomic symbols as in figure 1).

Table 1. Crystallographic data for the two structural forms of YbFe_6Ge_6 .

YCo ₆ Ge ₆ -type						
Atom	Site	Point symmetry	<i>x</i>	<i>y</i>	<i>z</i>	Occupancy
Yb	1a	6/ <i>mmm</i>	0	0	0	0.5
Fe	3g	<i>mmm</i>	$\frac{1}{2}$	0	$\frac{1}{2}$	1.0
Ge	2c	$\bar{6}m2$	$\frac{1}{3}$	$\frac{2}{3}$	0	1.0
Ge	2e	6 <i>mm</i>	0	0	0.307(5)	0.5
HfFe ₆ Ge ₆ -type						
Yb	1a	6/ <i>mmm</i>	0	0	0	1.0
Fe	6i	2 <i>mm</i>	$\frac{1}{2}$	0	0.2531(3)	1.0
Ge	2c	$\bar{6}m2$	$\frac{1}{3}$	$\frac{2}{3}$	0	1.0
Ge	2d	$\bar{6}m2$	$\frac{1}{3}$	$\frac{2}{3}$	$\frac{1}{2}$	1.0
Ge	2e	6 <i>mm</i>	0	0	0.344(1)	1.0

a very clear signal in the susceptibility with an onset around 65 K and a peak at 42 K. No such behaviour was observed in the ac-susceptibility of Y-type YbFe_6Ge_6 .

3.2. Neutron powder diffraction

In figure 5 we show the neutron diffraction patterns obtained at 4 K on the two forms of YbFe_6Ge_6 and in figure 6 we show the low-angle regions of the patterns obtained at 80 and 4 K on Y-type YbFe_6Ge_6 and at 4 K on H-type YbFe_6Ge_6 . The magnetic order of the Fe sublattice at 80 K in both forms of YbFe_6Ge_6 is along the crystal *C*-axis and is indicated by the magnetic peak (marked ‘M’) at $2\theta = 22.4^\circ$. This is the (101) peak in H-type YbFe_6Ge_6 and $(10\frac{1}{2})$ in Y-type YbFe_6Ge_6 . The $[0\ 0\ \frac{1}{2}]$ propagation vector of the Y-type YbFe_6Ge_6 magnetic structure reflects the factor of two difference in the *C* lattice parameters of the H-type and Y-type cells. At 4 K, the pattern of H-type YbFe_6Ge_6 shows a strong magnetic peak at $2\theta = 10.7^\circ$ which

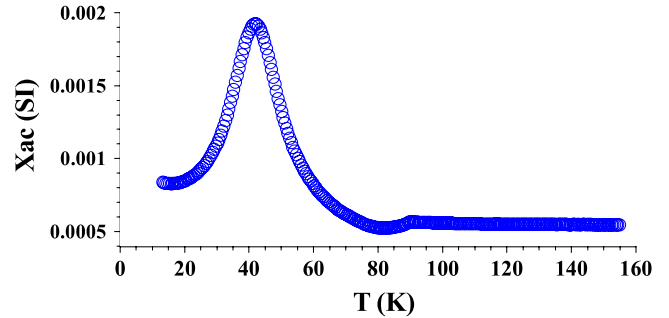


Figure 4. ac-susceptibility of H-type YbFe_6Ge_6 , obtained at a frequency of 137 Hz and an ac magnetic field of $700\ \text{A m}^{-1}$ (rms).

is the (001) peak. Below 65 K the intensity of the magnetic (001) peak increases and in figure 7 we show the temperature dependence of the (001) intensity. The growth of the (001) peak indicates that the spin reorientation of the Fe moments away from the hexagonal *C*-axis commences at 65 K and is more or less complete by 25 K. We note that the 4 K pattern of Y-type YbFe_6Ge_6 also shows a weak magnetic intensity at $2\theta = 10.7^\circ$ which indexes as $(00\frac{1}{2})$. This suggests that a very small (~ 5 wt%) cross-contamination of H-type phase in the Y-type sample is present, although a small reorientation of the Fe moments in Y-type YbFe_6Ge_6 away from the hexagonal *C*-axis cannot be definitively ruled out. However, as we shall see later, our Mössbauer work strongly suggests that any reorientation of the Fe moments in the Y-type form of YbFe_6Ge_6 away from the hexagonal *C*-axis is insignificant.

The refined Fe magnetic moment at room temperature is $1.42(10)\ \mu_B$ with the Fe moments directed along the *C*-axis. Our refinement of the 4 K neutron diffraction pattern of H-type YbFe_6Ge_6 yields Fe magnetic moments of $1.62(30)\ \mu_B$, lying at an angle of $69(12)^\circ$ from the *C*-axis. This angle is larger than the values of $56(3)^\circ$ and $64(3)^\circ$ reported by Mazet and Malaman [19]. The use of powder samples precludes the

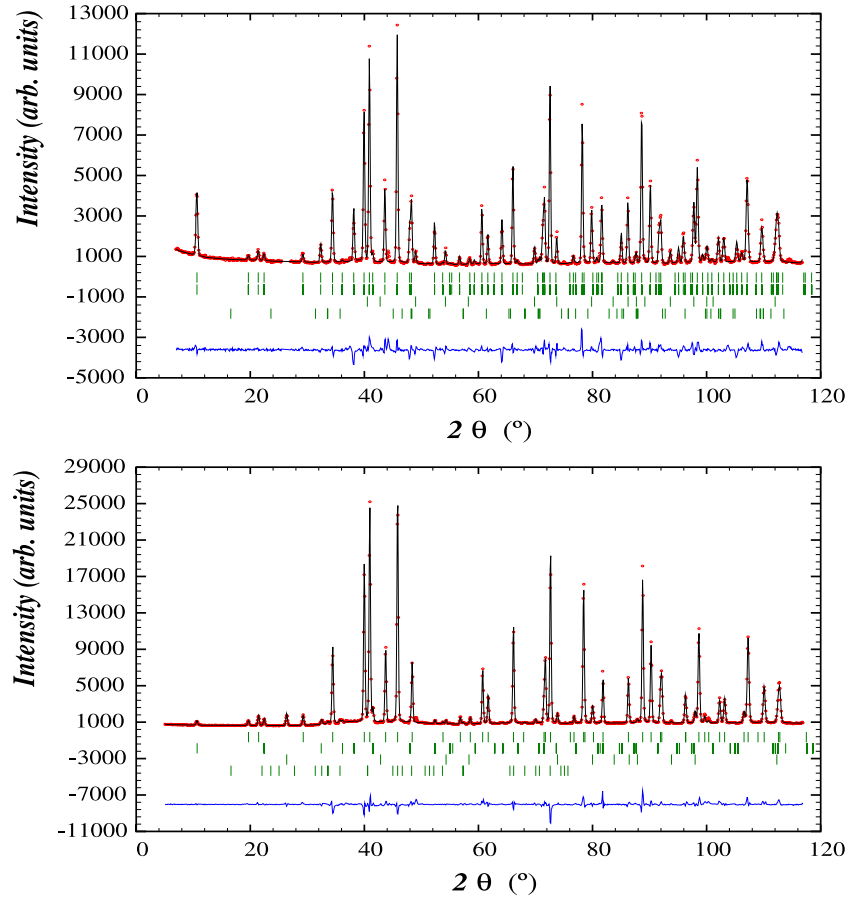


Figure 5. Neutron powder diffraction patterns of the H-type (top) and Y-type (bottom) forms of YbFe_6Ge_6 , obtained at 4 K with $\lambda = 1.5049(1) \text{ \AA}$. The Bragg markers (top to bottom) refer to the nuclear scattering from the YbFe_6Ge_6 phase, the magnetic scattering from the Fe sublattice, and the impurity phases (see the text).

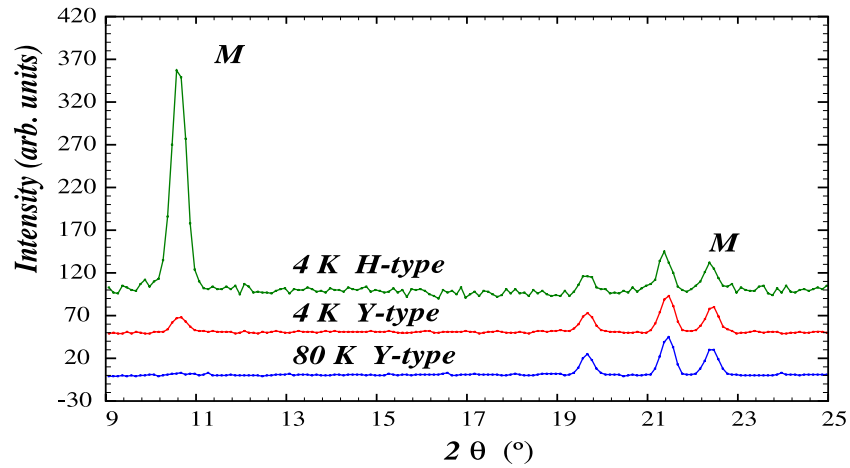


Figure 6. A comparison of the low-angle regions of the neutron powder diffraction patterns of H-type and Y-type YbFe_6Ge_6 , obtained at 4 and 80 K. The magnetic peaks are marked ‘M’.

determination of the azimuthal orientation of the Fe magnetic moments [24]. The conventional refinement R-factors (%) are: $R(\text{Bragg}) = 7.1$, $R(\text{F-struct.}) = 6.3$ and $R(\text{mag}) = 13.7$.

Our refinement of the 4 K neutron diffraction pattern of Y-type YbFe_6Ge_6 yields Fe magnetic moments of $1.56(40) \mu_B$, lying along the C-axis, assuming the more likely case of a slight cross-contamination of H-type phase in the Y-type

sample. The conventional refinement R-factors (%) are: $R(\text{Bragg}) = 4.7$, $R(\text{F-struct.}) = 2.8$ and $R(\text{mag}) = 10.2$.

3.3. ^{57}Fe Mössbauer spectroscopy

In figure 8 we show the ^{57}Fe Mössbauer spectra of H-type and Y-type YbFe_6Ge_6 , obtained at 12 K. The Y-type spectrum is

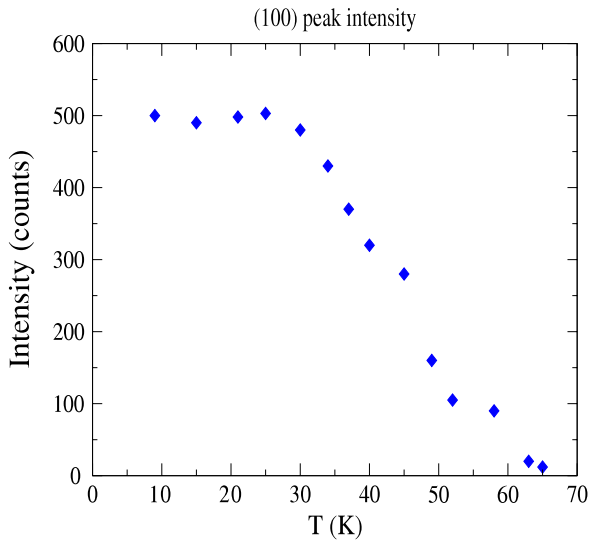


Figure 7. Temperature dependence of the intensity of the magnetic (001) peak seen in the neutron powder diffraction pattern of H-type YbFe_6Ge_6 .

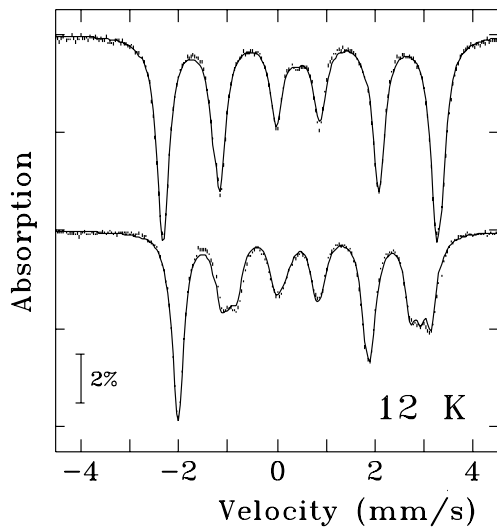


Figure 8. ^{57}Fe Mössbauer spectra of Y-type (top) and H-type (bottom) YbFe_6Ge_6 , obtained at 12 K.

well fitted with a single, magnetically-split sextet whereas the H-type spectrum requires three such sextets. These spectra indicate that the Fe moments in the Y-type phase remain ordered along, or very close to, the crystal C -axis, which leaves all Fe sites magnetically equivalent. By contrast, the splitting of the H-type spectrum shows that the Fe moments are ordered well away from the hexagonal C -axis, thereby splitting the 6i Fe sites into three magnetically inequivalent groups in the ratio 2:2:2.

In figure 9 we show the full series of ^{57}Fe Mössbauer spectra of H-type YbFe_6Ge_6 . Above about 60 K the spectra are well fitted with a single, magnetically-split sextet with a hyperfine field of 14.98(1) T at room temperature. This field, combined with the Fe magnetic moment of 1.42(10) μ_B deduced from the neutron diffraction measurements, yield

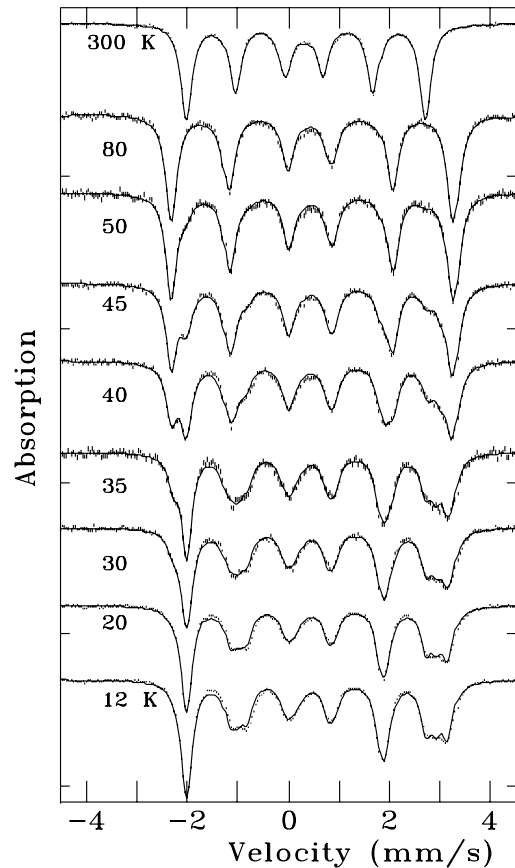


Figure 9. ^{57}Fe Mössbauer spectra of H-type YbFe_6Ge_6 .

a field-moment conversion factor of 10.55(75) T/ μ_B . The single-sextet nature of the spectra obtained above 60 K indicates that the Fe magnetic order is along the hexagonal C -axis above 60 K in both forms of YbFe_6Ge_6 .

Below 60 K the ^{57}Fe Mössbauer spectra of H-type YbFe_6Ge_6 split into three, equal-area sextets as the Fe moments reorient away from the crystal C -axis. Unlike the earlier study by Mazet and Malaman [19], we did not need to add a fourth sextet to fit these spectra. The temperature dependences of the hyperfine magnetic fields (B_{hf}) for the three Fe components are shown in figure 10. The effect of the spin reorientation is quite clear and will be discussed below in terms of anisotropic contributions to the hyperfine field.

By contrast, the ^{57}Fe spectrum of Y-type YbFe_6Ge_6 remains a single, magnetically-split sextet down to 4 K, with no signs of any splitting or additional broadening which might signal a significant spin reorientation. In figure 11 we show the temperature dependence of the fitted linewidth of the ^{57}Fe Mössbauer spectra of Y-type YbFe_6Ge_6 . The monotonic temperature dependence of the ^{57}Fe hyperfine field in Y-type YbFe_6Ge_6 is also shown in figure 10. The ^{57}Fe hyperfine fields in the two phases track together above the spin-reorientation temperature of H-type YbFe_6Ge_6 as all Fe moments are ordered along the hexagonal C -axis.

The temperature dependences of the electric quadrupole shifts (QS_{mag}) for the three Fe components in the low-temperature Mössbauer spectra of H-type YbFe_6Ge_6 are shown

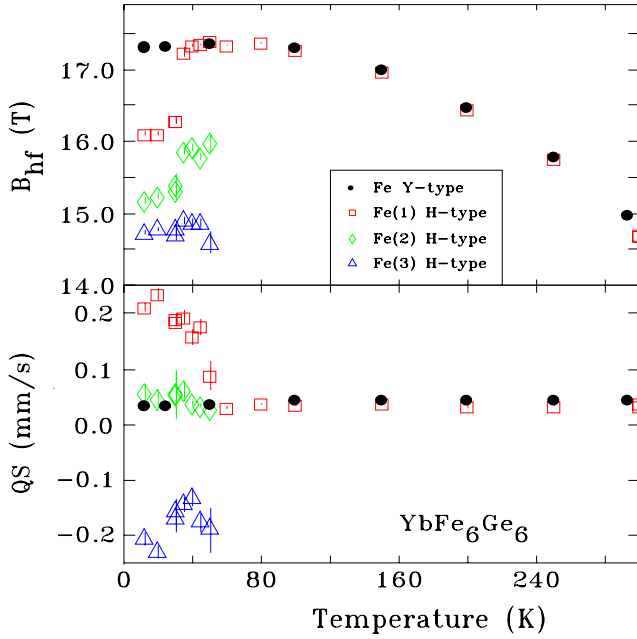


Figure 10. ^{57}Fe hyperfine fields and quadrupole shifts in the Y-type and H-type forms of YbFe_6Ge_6 .

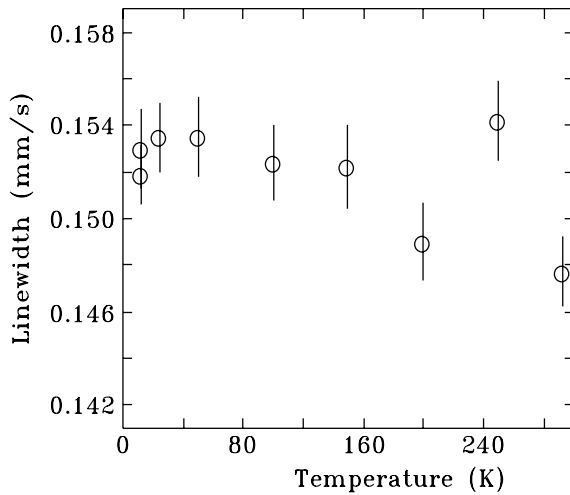


Figure 11. Temperature dependence of the ^{57}Fe Mössbauer spectral linewidth (half-width at half-maximum intensity) of Y-type YbFe_6Ge_6 .

in figure 10. Once again, the effect of the spin reorientation in H-type YbFe_6Ge_6 is quite clear. The possibility of a slight canting of the Fe order away from the C -axis in Y-type YbFe_6Ge_6 is not observed by Mössbauer spectroscopy. The 3-fold splitting of the Fe spectra in H-type YbFe_6Ge_6 due to the spin reorientation reflects the changing orientation of the hyperfine field within the principal frame of the electric field gradient (EFG). The reductions in hyperfine field, amounting to 1–3 T, are due to anisotropic contributions to the net hyperfine field [25] (see below).

At this point it is important to identify the principal axes of the EFG at the Fe sites. The point group of the Fe sites in H-type YbFe_6Ge_6 is $2mm$ with the 2-fold axis being the

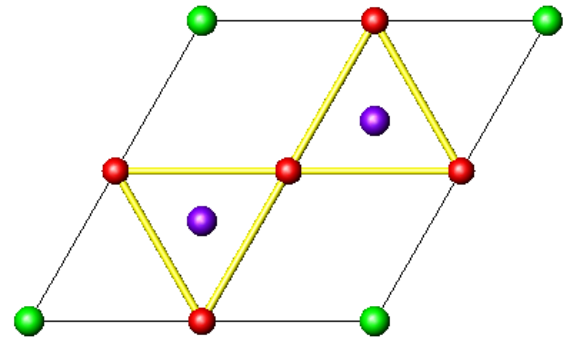


Figure 12. Planar arrangement of the Fe sites in H-type YbFe_6Ge_6 . (Yb = green, Fe = red and Ge = purple.)

crystal C -axis. The planar arrangement of the 6i Fe sites in H-type YbFe_6Ge_6 is shown in figure 12. One of the EFG axes must lie along the C -axis, with the other two axes being in the hexagonal plane. One of these planar axes is perpendicular to the local mirror plane and the other lies in the mirror plane. Unfortunately, we cannot tell which axis is which *a priori*. However, we can use the measured quadrupole splitting of the Fe spectrum in the paramagnetic regime together with the convention

$$0 \leq \eta \leq 1, \quad (1)$$

where η is the local EFG asymmetry parameter, to identify the EFG axes. Above the magnetic ordering temperature, the ^{57}Fe Mössbauer spectrum in H-type YbFe_6Ge_6 is a simple quadrupole-split doublet with a splitting of $\pm 0.289(1) \text{ mm s}^{-1}$ (the sign cannot be determined from a simple doublet). Below the ordering temperature but *above* the spin-reorientation temperature, the quadrupole shift is $+0.036(3) \text{ mm s}^{-1}$. These data, together with the η convention above, allow us to identify the x -axis of the EFG as the crystal C -axis, in agreement with our previous point-charge calculations [26] and also in agreement with the findings of Mazet and Malaman [19].

The splitting of the two lines in a quadrupole doublet is given by

$$\Delta = \frac{eQV_{ZZ}}{2} \sqrt{\left(1 + \frac{\eta^2}{3}\right)}, \quad (2)$$

where Q is the electric quadrupole moment of the excited nuclear state of ^{57}Fe and V_{ZZ} is the principal term of the EFG tensor. The electric quadrupole parameter in a magnetically-split sextet manifests itself as shifts in the lines, leading to an asymmetric sextet, and is given by

$$QS_{\text{mag}} = \frac{eQV_{ZZ}}{4} [3 \cos^2 \theta - 1 + \eta \sin^2 \theta \cos(2\phi)], \quad (3)$$

where θ and ϕ are the polar and azimuthal angles of the magnetic hyperfine field \mathbf{B}_{hf} in the EFG frame. Because the principal Z -axis of the EFG is perpendicular to the crystal's hexagonal C -axis we shall distinguish the crystallographic orientation of the magnetic moments by writing the crystallographic orientation in terms of the polar and azimuthal angles α and β defined relative to the crystal C and A axes. Clearly, there are simple trigonometric relationships between (θ, ϕ) and (α, β) .

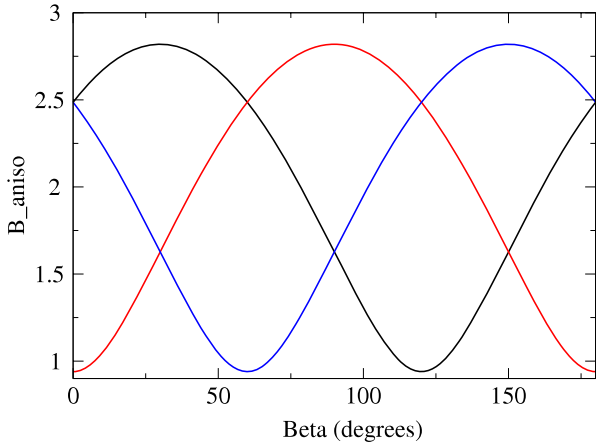


Figure 13. Angular dependence of the magnitude of the anisotropic contribution to the hyperfine field for the three ^{57}Fe sub-sites in H-type YbFe_6Ge_6 .

The above Mössbauer data allow us to deduce an electric field gradient at the ^{57}Fe nucleus of $eQV_{ZZ} = -0.53(5) \text{ mm s}^{-1}$ and an asymmetry parameter of $\eta = 0.73(7)$. These values are in excellent agreement with the corresponding values deduced by Mazet and Malaman [19], namely $eQV_{ZZ} = -0.50(6) \text{ mm s}^{-1}$ and $\eta = 0.7(1)$.

The magnetic hyperfine field at the ^{57}Fe nucleus comprises an isotropic term \mathbf{B}_{iso} , which is predominantly due to a Fermi-contact interaction, and an anisotropic term $\mathbf{B}_{\text{aniso}}$ which may arise from sources such as neighbouring dipole moments, the effects of covalent bonding and orbital components of the Fe moment. The net hyperfine field is the vector sum of these two contributions (the isotropic field is collinear with the Fe atomic magnetic moment but the anisotropic term need not be so). As shown in [25], the anisotropic field can be written in the form

$$\mathbf{B}_{\text{aniso}} = \mathbf{A}_p \left[\sum \mathbf{u}_i (\mu_i \cdot \mathbf{u}_i) - \frac{1}{3} \sum \mu_i \right]. \quad (4)$$

In figure 13 we show the azimuthal angular dependences of the magnitudes of the anisotropic contributions to the ^{57}Fe hyperfine field at the three Fe sub-sites, calculated using equations (4). The observed ^{57}Fe hyperfine fields are fully consistent with these contributions.

In figure 14 we show the azimuthal angular dependences of the electric quadrupole shifts at the three Fe sub-sites, calculated using equations (3). The observed ^{57}Fe electric quadrupole shifts are consistent with these calculations. The two options in the electric quadrupole shift figure refer to the two options for the orientations of the Y and Z axes of the EFG within the hexagonal plane.

On the basis of the ^{57}Fe Mössbauer results we cannot determine the exact orientation of the Fe sublattice magnetization in H-type YbFe_6Ge_6 , if we assume that the Fe moments remain collinear. However, our measured quadrupole shifts at the three Fe sub-sites allow us to say that the canting angle relative to the hexagonal C -axis (i.e. α) must be at least 60° but most likely less than 90° . This is fully consistent with our neutron diffraction refinements. Furthermore, the fact that

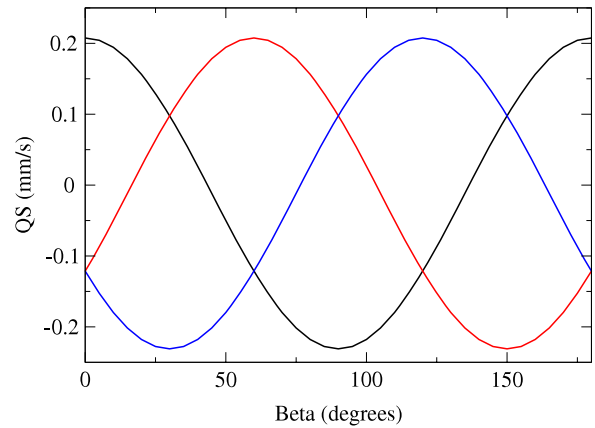
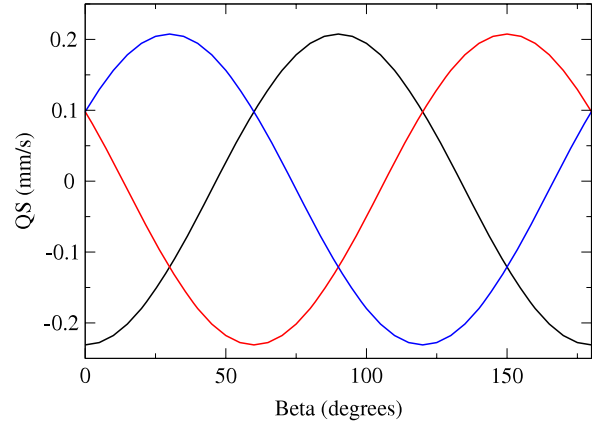


Figure 14. Angular dependences of the electric quadrupole shift (axes option 1 (top) and 2 (bottom)) for the three ^{57}Fe spectral components in H-type YbFe_6Ge_6 .

we see three distinct, equal-area sextets rules out azimuthal angles (i.e. β) along symmetry directions i.e. $0^\circ, 30^\circ, 60^\circ, 90^\circ$, etc as these would produce a two-fold splitting in the area ratio 2:1. Azimuthal order along a symmetry direction is also ruled out by the anisotropic hyperfine field dependences shown in figure 13.

3.4. ^{170}Yb Mössbauer spectroscopy

In many compounds containing Yb, the Yb ion is divalent, in order to fill its 4f shell, rather than trivalent as is the norm for rare-earth ions. As a result, Yb compounds can exhibit a variety of mixed-valent or intermediate-valence effects. One possible factor which may be responsible for the different magnetic behaviours of the two forms of YbFe_6Ge_6 is related to the electronic structures in these compounds and it is important to identify the Yb valence. In figure 15 we show the ^{170}Yb Mössbauer spectrum (at 5 K) of Y-type YbFe_6Ge_6 . The spectrum is a paramagnetic quadrupole triplet with a quadrupole splitting of $+9.58(10) \text{ mm s}^{-1}$. This is clear evidence of a trivalent Yb ion since Yb^{2+} has a full 4f electron shell and hence no 4f contribution to the EFG at the ^{170}Yb nucleus.

We may use the results of our recent ^{155}Gd Mössbauer study of GdFe_6Ge_6 [27] to estimate the lattice contribution to the EFG at the ^{170}Yb nucleus in YbFe_6Ge_6 . We

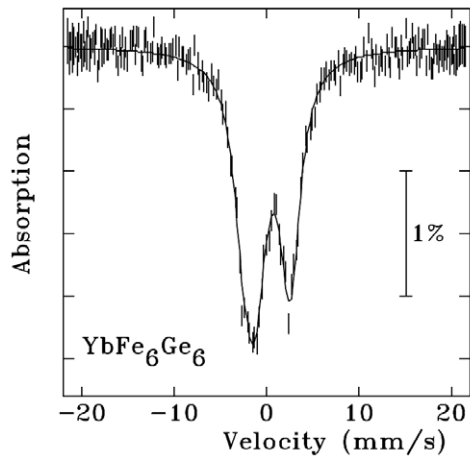


Figure 15. ^{170}Yb Mössbauer spectrum of Y-type YbFe_6Ge_6 , obtained at 5 K.

note here that GdFe_6Ge_6 also forms in the hexagonal Y-type structure. As shown in our paper on GdFe_6Ge_6 , the principal component of the EFG at the ^{155}Gd nucleus is $V_{ZZ} = +(5.8 \pm 2.1) \times 10^{20} \text{ V m}^{-2}$. This value represents contributions from sources external to the 4f shell since Gd^{3+} is an S-state ion with no 4f contribution to the EFG. If we make a reasonable ‘first-order’ assumption that the external EFG at the R site remains constant across the RFe_6Ge_6 series then the ^{155}Gd value of V_{ZZ} leads to a lattice EFG of $+0.44(16) \text{ mm s}^{-1}$ at the ^{170}Yb nucleus, only about 5% of our observed value of $+9.58(10) \text{ mm s}^{-1}$, indicating that the parent Yb ion in YbFe_6Ge_6 is trivalent. For the benefit of the reader we note that a Mössbauer velocity of 1 mm s^{-1} converts to $4.503 \times 10^{-26} \text{ J}$ for the 84.25 keV Mössbauer transition in ^{170}Yb . Also, the electric quadrupole moment of the excited Mössbauer state in ^{170}Yb is $-2.11(11) \text{ b}$. Once again, we refer the reader to our review article on R-isotope Mössbauer transitions for a discussion of ^{170}Yb Mössbauer spectroscopy [21].

In an attempt to explain the observation of the spin reorientation in H-type YbFe_6Ge_6 Mazet and Malaman [19] considered the possibility of valence effects at the Yb ion. The measured ^{57}Fe hyperfine fields of 14.6–17.6 T at 4 K lie in the range expected for a trivalent R ion in RFe_6Ge_6 , as shown in their paper on the H-type MFe_6Ge_6 compounds with $\text{M} = \text{Sc}, \text{Ti}, \text{Zr}, \text{Hf}$ and Nb [28]. Furthermore, their analysis of the lattice parameters of YbFe_6Ge_6 showed no anomalous behaviour when compared systematically with data for other RFe_6Ge_6 compounds where the R ion is known to be trivalent. Thus, Mazet and Malaman quite rightly concluded that the Yb ion in H-type YbFe_6Ge_6 has a valence of 3+ or close to that value.

3.5. Discussion

In a XANES study of a single crystal of H-type YbFe_6Ge_6 , Avila *et al* [20] demonstrated that Yb is indeed trivalent in this compound. Our lattice parameters for the two forms of YbFe_6Ge_6 show no anomaly related to valence: the C

parameters and hence the cell volumes differ by a factor of two, as expected from the crystallographic models shown in figures 1–3. Furthermore, the substantial quadrupole splitting we observe in our ^{170}Yb Mössbauer spectrum of Y-type YbFe_6Ge_6 clearly suggests Yb^{3+} .

A major thrust of the work reported by Avila *et al* [20] was to try to explain why the Fe sublattice in H-type YbFe_6Ge_6 undergoes a spin reorientation. Although spin reorientations of the magnetic structure in the RFe_6Ge_6 and RFe_6Sn_6 series are rare, it is perhaps not so surprising that such a reorientation is observed in YbFe_6Ge_6 , where the R ion is quite small, reflecting the well-known ‘lanthanide contraction’. Thus, YbFe_6Ge_6 is more closely related to the underlying FeGe structure than those RFe_6Ge_6 and RFe_6Ge_6 compounds formed with larger R ions, which generally crystallize in related orthorhombic structures. As mentioned earlier, the Fe sublattice in FeGe undergoes a spin reorientation away from the hexagonal C-axis below 55 K and forms a double-cone structure at low temperatures [15]. What is perhaps surprising is the lack of a significant reorientation of the Fe magnetic order in Y-type YbFe_6Ge_6 . It is possible that this difference in intrinsic magnetic behaviour stems from differences in the electronic band structures of the Fe sublattices in the two forms of YbFe_6Ge_6 . The fact that two of the atomic sites in Y-type YbFe_6Ge_6 are half-filled may also play a role in maintaining the uniaxial Fe anisotropy in that compound. The resolution of this problem awaits band structure calculations.

4. Conclusions

We have studied the crystal and magnetic structures of the two crystallographic forms of YbFe_6Ge_6 by Mössbauer spectroscopy (^{57}Fe and ^{170}Yb) and neutron powder diffraction. The Fe sublattice orders antiferromagnetically at 485(2) K. In the HfFe_6Ge_6 form of YbFe_6Ge_6 , the Fe sublattice undergoes a spin reorientation away from the crystal C-axis, commencing at around 65 K. By 4 K, the Fe moments lie close to the hexagonal plane but not in that plane. In contrast, the Fe sublattice in the YCo_6Ge_6 form of YbFe_6Ge_6 remains ordered along the C-axis, at least to within about 10° . This observation of two closely related crystallographic forms of YbFe_6Ge_6 , whose intrinsic magnetic behaviours differ, provides a simple explanation for the unusual splitting in the ^{57}Fe Mössbauer spectra of YbFe_6Ge_6 , previously reported by Mazet and Malaman [19].

Acknowledgments

We are grateful to the staff at CNBC Chalk River, particularly I P Swainson, for their assistance during the neutron diffraction measurements. JMC acknowledges support from the Canada Research Chairs programme. Some of the work reported here was carried out while JMC was on the faculty of the University of New South Wales in Sydney. Financial support for various stages of this work was provided by the Australian Research Council, the University of New South Wales, the Natural Sciences and Engineering Research Council of Canada and Fonds Québécois de la Recherche sur la Nature et les

Technologies. The ^{170}Yb source activation was carried out by M Butler at the McMaster Nuclear Reactor, Hamilton, Ontario.

References

- [1] Cadogan J M and Ryan D H 2001 *J. Alloys Compounds* **326** 166–73
- [2] Chafik El Idrissi B, Venturini G and Malaman B 1991 *Mater. Res. Bull.* **26** 1331–8
- [3] Ryan D H and Cadogan J M 1996 *J. Appl. Phys.* **79** 6004–6
- [4] Buchholz W and Schuster H-U 1981 *Z. Anorg. Allg. Chem.* **482** 40–8
- [5] Dzyanyani R B, Bodak O I and Aksel'rud L G 1995 *Mater. Sci.* **31** 284–5
- [6] Venturini G, Welter R and Malaman B 1992 *J. Alloys Compounds* **185** 99–107
- [7] Venturini G 2006 *Z. Kristallogr.* **221** 511–20
- [8] Nikolaev V I, Yakimov S S, Dubovtsev I A and Gavrilova Z G 1965 *Sov. Phys.—JETP Lett.* **2** 235–7
- [9] Tomiyoshi S, Yamamoto H and Watanabe H 1966 *J. Phys. Soc. Japan* **21** 709–12
- [10] Haggström L, Ericsson T, Wäppling R and Karlsson E 1975 *Phys. Scr.* **11** 55–9
- [11] Beckman O, Carrander K, Lundgren L and Richardson M 1972 *Phys. Scr.* **6** 151–7
- [12] Sundström L J 1972 *Phys. Scr.* **6** 158–63
- [13] Stenström B and Sundström L J 1972 *Phys. Scr.* **6** 164–8
- [14] Forsyth J B, Wilkinson C and Gardner P 1978 *J. Phys. F: Met. Phys.* **8** 2195–202
- [15] Bernhard J, Lebech B and Beckman O 1984 *J. Phys. F: Met. Phys.* **14** 2379–93
- [16] Bernhard J, Lebech B and Beckman O 1988 *J. Phys. F: Met. Phys.* **18** 539–52
- [17] Nazareno H, Carabelli G and Calais J-L 1971 *J. Phys. C: Solid State Phys.* **4** 2052–63
- [18] Lebech B, Izyumov Yu A and Syromiatnikov V 1987 *J. Phys. C: Solid State Phys.* **20** 1713–28
- [19] Mazet T and Malaman B 2000 *J. Phys.: Condens. Matter* **12** 1085–95
- [20] Avila M A, Takabatake T, Takahashi Y, Bud'ko S L and Canfield P C 2005 *J. Phys.: Condens. Matter* **17** 6969–79
- [21] Cadogan J M and Ryan D H 2004 *Hyperfine Interact.* **153** 25–41
- [22] Rodríguez-Carvajal J 1993 *Physica B* **192** 55–69
- [23] Roisnel T and Rodríguez-Carvajal J 2001 *Mater. Sci. Forum* **378–381** 118–23
- [24] Shirane G 1959 *Acta Crystallogr.* **12** 282–3
- [25] Le Caër G, Malaman B, Venturini G and Kim I B 1982 *Phys. Rev. B* **26** 5085–96
- [26] Wang Y B, Wiarda D, Ryan D H and Cadogan J M 1994 *IEEE Trans. Magn.* **30** 4951–3
- [27] Cadogan J M, Ryan D H and Cashion J D 2007 *J. Phys.: Condens. Matter* **19** 216204
- [28] Mazet T, Isnard O and Malaman B 2000 *Solid State Commun.* **114** 91–96